

NON-LINEAR VACUUM POLARIZATION IN STRONG FIELDS

M. Gyulassy

Nuclear Science Division
Lawrence Berkeley Laboratory
University of California
Berkeley, CA 94720

This work was supported by the Director, Office of Energy Research, Division of Nuclear Physics of the Office of High Energy and Nuclear Physics of the U.S. Department of Energy under Contract W-7405-ENG-48.

NON-LINEAR VACUUM POLARIZATION IN STRONG FIELDS

M. Gyulassy

Nuclear Science Division
Lawrence Berkeley Laboratory
University of California
Berkeley, CA 94720

INTRODUCTION

A particularly interesting consequence of the Dirac equation and hole theory is the phenomenon of spontaneous e^+e^- pair creation in strong static electric fields¹⁻³. Normally, pair creation in a static field costs energy, $\Delta E = 2m_e - B$, where B is the binding energy of the electron. Consequently, spontaneous pair creation is normally a virtual process lasting only a short time, $\Delta t \sim 1/\Delta E = (2m_e - B)^{-1}$. This virtual process is called vacuum polarization in Quantum Electrodynamics (QED). However, if the external fields become so strong that $B \rightarrow 2m_e$, then $\Delta t \rightarrow \infty$, and the virtual pair can "materialize". In terms of QED this would be called real or on-shell vacuum polarization.

The necessary condition ($B \rightarrow 2m_e$) for real vacuum polarization has been estimated¹⁻³ to occur for very high nuclear charges $Z > Z_c \approx 175$. This range of Z is fortunately accessible via heavy ion collisions. In such high fields $Z \gg 1$ and relativistic non-linear effects are important.

While in the Dirac equation it is formally possible to increase Z indefinitely (for finite size nuclei), it is not clear a priori whether a full QED calculation allows arbitrary large fields and bindings. In particular, it could be that radiative corrections such as self-energy and vacuum polarization effects could increase so rapidly with Z that the diving condition, $B = 2m_e$, is significantly delayed or even prevented.

Even classically it could be that non-linear effects, unobserved in low field ($Z < 100$) experiments, could become important in the strong field limit $Z \rightarrow Z_c$. As an example of non-linear electrodynamics Rafelski, et al.⁴ applied the Born-Infeld⁵ Lagrangian to calculate $B(Z)$. In that theory there is an upper bound of $E_{BI} = 1.2 \times 10^{18}$ V/cm on the electric field strength. While the non-linearities do not prevent B from reaching $2m_e$, the critical charge was shifted to $Z_c > 200$, beyond the range accessible via heavy ion collisions. Later, Soff et al.⁶ showed that high precision experiments on muonic atoms require a lower bound on the maximum field strength $E^* > 100 E_{BI}$. In that case, classical non-linear effects could change Z_c by at most a few units. Therefore, this type of classical non-linear electrodynamics cannot prevent diving.

On the other hand, the QED calculations of Wichmann and Kroll⁷ showed that non-linear vacuum polarization screening has a singular derivative with respect to Z at $Z = 137$. This singularity was due to the assumed point nuclear charge distribution. Nevertheless, it indicated that vacuum polarization screening could be expected to grow rapidly with Z beyond 137 when finite nuclear size effects are taken into account. In this review, I focus on this aspect of non-linear vacuum polarization in strong fields. The basic question addressed is whether virtual pair creation (vacuum polarization) can screen the nuclear charge sufficiently to prevent real vacuum polarization (spontaneous e^+e^- production). As I show below, the answer is no.

The remainder of this review is organized as follows: The Wichmann-Kroll formalism for calculating the vacuum polarization density to first order in α but to all orders in $Z\alpha$ is derived. The most essential quantity is shown to be the electrons Green's function in these calculations. The method of constructing that Green's function in the field of finite radius nuclei is then presented.

Comparing the calculations with data on muonic atoms shows good agreement with data and gives us confidence in extending the calculations beyond $Z = 137$. The $1S_{1/2}$ shift is then calculated as $Z \rightarrow Z_c$. The main result is that the screening due to non-linear vacuum polarization remains small all the way up to Z_c . In terms of an effective screening charge, Q_{eff} , the vacuum screens the nuclear charge by only $Q_{eff} \approx e/20$ at $Z_c \approx 175$. Therefore, vacuum polarization cannot prevent diving and is nonsingular in the strong field limit. Finally, it is shown that the charge density of the overcritical vacuum ($Z > Z_c$) is highly localized and represents the smooth continuation of the He-like charge density for $Z < Z_c$.

WICHMANN-KROLL FORMALISM

The first step is to write the vacuum polarization charge density as

$$\rho_{VP}(x) = -\frac{|e|}{2} \langle 0 | [\psi^\dagger(x), \psi(x)] | 0 \rangle, \quad (1)$$

where ψ is the electron field operator and $|0\rangle$ is the vacuum state. It is necessary to write the commutator of ψ^\dagger and ψ to insure correct charge conjugation properties. In general, $\psi(x)$ and the photon field $A_\mu(x)$ satisfy coupled Dirac and Maxwell field equations. However, in order to calculate the vacuum polarization density to lowest order α but to all orders in $Z\alpha$, it is possible to decouple these equations. To lowest order in α , $\psi(x)$ satisfies the Dirac equation

$$(i\cancel{\partial} - Z\alpha V(r)\gamma_0 - m_e)\psi(x) = 0, \quad (2)$$

with the external c-number field $A_{ex}^\mu = \delta_{\mu 0} Ze V(r)$ satisfying the classical Maxwell equations $\nabla^2 V = -\rho_{ex}$. To solve eq. (2), $\psi(x)$ can be expanded in terms of the complete set of positive and negative energy eigenfunctions, $\psi_E(x)$, of the Dirac equation

$$\psi(x) = \sum_{E > E_F} \psi_E(x) b_E + \sum_{E < E_F} \psi_E(x) d_E^\dagger, \quad (3)$$

with b_E and d_E being the anticommuting destruction operators of electrons and positrons. The sum over spin projections is implicit in eq. (3). Also E_F is the Fermi energy, $m_e \approx E_F < m_e - B(1S_{1/2})$. Equation (3) defines the Furry bound interaction picture. We can now evaluate eq. (1) giving

$$\rho_{VP}(x) = \frac{|e|^2}{2} \left\{ \sum_{E > E_F} |\psi_E(x)|^2 - \sum_{E < E_F} |\psi_E(x)|^2 \right\}. \quad (4)$$

As $Z \rightarrow 0$, $\rho_{VP} \rightarrow 0$ due to the symmetry between positive and negative energy plane wave solutions.

The main trick in the Wichmann-Kroll approach is to calculate $|\psi(x)|^2$ from the residues of the electron Green's function. Observe that

$$G(x, y; -) = \sum_E \frac{\psi_E(x) \psi_E^\dagger(y)}{E - i0} \quad (5)$$

is a solution to the equation

$$(H_x - \omega)G(x, y; \omega) = \delta^3(x - y) \quad (6)$$

with $H_x = -i\alpha \cdot \nabla + \beta m_e + V(r)$, because $\{u_E(x)\}$ form a complete set of solutions of the Dirac equation, $(H - E)u_E = 0$. For an isolated pole of G , it is obvious from eq. (5) that

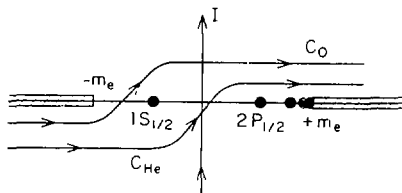
$$\begin{aligned} |u_E(x)|^2 &= - \operatorname{Res}_{\omega=E} \operatorname{Tr} G(x, x; \omega) \\ &= \int_{C_E} \frac{d\omega}{2\pi i} \operatorname{Tr} G(x, x; \omega), \end{aligned} \quad (7)$$

where C_E is a clockwise contour around E . Therefore, we can express the vacuum polarization density from eq. (4) as

$$\rho_{VP}(x) = \frac{|e|^4}{2} \left\{ \int_{C_+} + \int_{C_-} \right\} \frac{d\omega}{2\pi i} \operatorname{Tr} G(x, x; \omega), \quad (8)$$

where the contour C_+ goes clockwise around all the positive energy singularities of G and where C_- goes counter-clockwise around all the negative energy singularities. Noting that G has no singularities away from the real axis, these contours can be rotated for convenience so that $1/2(C_+ + C_-) = C_F$, where the Feynman contour C_F is illustrated in Fig. 1.

We obtain finally the contour integral representation of ρ_{VP} as



XBL 747-3588

Fig. 1. Singularities of Green's function in complex energy plane. Contour $C_0 = C_F$ in eq. (9) and C_{He} is for eq. (31).

$$\begin{aligned} \rho_{VP}(x) &= |e| \int_{C_F} \frac{d\omega}{2\pi i} \text{Tr}G(x, x; \omega) \\ &= i|e| \text{Tr}(S_F(x, x')\gamma_0) \Big|_{x' \rightarrow x} \end{aligned} \quad (9)$$

where $iS_F(x, x') = \langle 0 | T(\psi(x)\bar{\psi}(x')) | 0 \rangle$ is the familiar Feynman propagator⁹. What has been accomplished by rotating the contours into C_F is a relation between ρ_{VP} and the equal time-equal space point value of the Feynman propagator. This is useful because we know how to draw Feynman diagrams for $S_F(x, x')$ and consequently we obtain a diagrammatic expansion of $\rho_{VP}(x)$:

$$\rho_{VP}(x) = \text{Diagram 1} + \text{Diagram 2} + \text{Diagram 3} + \dots \quad (10)$$

where \rightarrow is the diagram corresponding to the amplitude to propagate an electron from x' to x in the absence of interactions. Thus, $\rho_{VP}(x)$ can be pictured as a "besoffenes" electron that staggers from point x back to x occasionally drinking (☉) "einen Schluck edlen Rheinweins".

Because the trace of an odd number of γ matrices vanishes, only terms with an odd number of external interactions (or Schluck) survive [note the extra γ_0 at the point x from eq. (9)]. This is Furry's theorem, which guarantees that only odd powers of Z_3 occur in the expansion of ρ_{VP} .

$$\rho_{VP}(x) = Z_3 \cdot 1 + (Z_3)^3 \cdot 3 + \dots \quad (11)$$

Having a diagrammatic expansion of ρ_{VP} we can see that not all diagrams are free from ambiguity. In particular, the first order diagram diverges quadratically since the internal loop integration, $\int d^4p \text{Tr}[\gamma_0 S_F(p)\gamma_0 S_F(p+q)]$, behaves in the ultraviolet limit as $\int d^4p/p^2 \rightarrow \infty^2$. Actually, if we look in more detail (see Bjorken and Drell⁹, for example) imposing gauge invariance reduces the degree of divergence such that $\rightarrow \infty$. This remaining divergence can be removed because it merely renormalizes the bare nuclear charge, $Z_3 \rightarrow Z_3^{\text{reg}}$. To see this it is convenient to regulate the expression for ρ_1 according to the Pauli-Villars method⁹

$$\rho_1^{\text{reg}} = \lim_{M \rightarrow \infty} [\rho_1(m_e) - \rho_1(M)] \quad (12)$$

In eq. (12) $\rho_1(M)$ corresponds to the first order diagram with the electron mass replaced by M . The regulated first order density in momentum space is then found to be⁹

$$Z_{\alpha 0}^{\text{reg}}(q) = Z_{\alpha 0}^{\text{bare}}(q) \times \left\{ -\frac{\alpha}{3\pi} \log \frac{M^2}{m_e^2} + \frac{2\alpha}{\pi} \int_0^1 dx x(1-x) \log \left[1 + \frac{q^2 x(1-x)}{m_e^2} \right] \right\}. \quad (13)$$

The total charge density to order $\alpha(Z_1)$ is then

$$Z_{\alpha 0}^{\text{ex}}(q) = Z_{\alpha 0}^{\text{bare}}(q) + Z_{\alpha 0}^{\text{reg}}(q). \quad (14)$$

We now see that the $\log M^2$ term in eq. (13) simply rescales the bare nuclear charge density. The sign of this effect is in accord with our intuition that vacuum polarization should screen the nuclear charge. The second term vanishes in the $q \rightarrow 0$ limit, which implies that it contains no net charge. This second term is the finite physical part of the first order (Uehling) VP density. It is interesting to note the famous "asymptotic slavery" property of QED in eq. (14). As $q^2 \rightarrow \infty$,

$$Z_{\alpha 0}^{\text{ex}}(q) \rightarrow Z_{\alpha 0}^{\text{bare}}(q) \left\{ 1 - \frac{\alpha}{3\pi} \log \frac{M^2}{m_e^2} + \frac{\alpha}{3\pi} \log \frac{q^2}{m_e^2} \right\}. \quad (15)$$

Therefore, with increasing momentum transfers, corresponding to smaller r , the strength of the nuclear charge increases. Expressed in coordinate space, Blomqvist¹⁰ found the small r behavior of the screened nuclear potential to be

$$Z_1 V(r) = -\frac{Z_1}{r} \left\{ 1 + \frac{2}{3} \left[\log \frac{1}{r} - 1.41 + O(m_e r) \right] \right\}. \quad (16)$$

Equation (16) shows explicitly that the strength of the potential increases in the small $r \ll r_e$ limit. (For large r , the Uehling potential falls off exponentially.)

Having reviewed the first order $\alpha(Z_1)$ part of the VP density, I turn next to the non-linear parts of order $\alpha(Z_1)^{n-3}$. From the diagrams in eq. (10), the ultraviolet behavior of the n^{th} order density goes as $\sim \int d^4 p / p^{n+1}$. For order $\alpha(Z_1)^{n-5}$ this is manifestly finite. For order $\alpha(Z_1)^3$ it shows an apparent logarithmic divergence. However, gauge invariance eliminates this divergence and all higher order diagrams $\alpha(Z_1)^{n-3}$ are finite and well behaved for bounded external potentials. Thus, only the first order diagram requires special care. Since we now know the analytic form of first order density, the higher order density can be calculated from eq. (9) simply by subtracting the first order Green's function.

In order to carry out this subtraction, it is convenient for spherically symmetric systems to expand the Green's function in eigenfunctions of the Dirac angular momentum $K = \gamma_0(\mathbf{j} \cdot \mathbf{L} + 1)$. The eigenvalues are $k = \pm(j + 1/2)$ in terms of the total angular momentum j . Details of this expansion can be found in Ref. 11. For the trace needed in eq. (9), the expansion is particularly simple

$$\text{Tr } G(\mathbf{x}, \mathbf{x}; \omega) = \sum_{j=1/2, 3/2, \dots} \frac{2j+1}{4\pi} \text{Tr} \left[G_{k=j+1/2}(r, r'; \omega) + G_{k=-j-1/2}(r, r'; \omega) \right] \quad (17)$$

where $G_k(r, r'; \omega)$ is the radial Green's function, that satisfies¹¹

$$\begin{bmatrix} m_e + V(r) - \omega & -\frac{1}{r} \frac{d}{dr} r + \frac{k}{r} \\ \frac{1}{r} \frac{d}{dr} r + \frac{k}{r} & -m_e + V(r) - \omega \end{bmatrix} G_k(r, r'; \omega) = \frac{\delta(r-r')}{rr'} \quad (18)$$

With eq. (17) we can now define the vacuum polarization density due to a particular angular momentum j as

$$\rho_j(r) = |e|^2 \frac{(2j+1)}{4\pi} \int_{C_F} \frac{d.}{2-i} \text{Tr} [G_{j+1/2}(r, r'; \omega) + G_{-j-1/2}(r, r'; \omega)] \quad (19)$$

It is straightforward to show^{8c} that $\rho_j(r)$ is an odd function of Z as required byurry's theorem.

Converting eq. (18) into an integral equation, the first order contribution for a given k is

$$\text{Tr } Z : G_k^1(r, r'; \omega) = Z \int_0^\infty dr' r'^2 V(r') \text{Tr} [G_k^0(r, r'; \omega) G_k^0(r', r'; \omega)] \quad (20)$$

where G_k^0 is the free space radial propagator involving spherical Bessel functions^{8, 11}.

Finally, the expression for the non-linear $(Z \cdot n)^3$ vacuum polarization density for a given j can be written as

$$\rho_j^{3+}(r) = |e|^2 \frac{2j+1}{4\pi} \int_{C_F} \frac{d.}{2-i} \times \text{Tr} \left[G_{j+1/2}(r, r'; \omega) + G_{-j-1/2}(r, r'; \omega) - 2Z : G_{j+1/2}^1(r, r'; \omega) \right] \quad (21)$$

This expression is now finite and well behaved. In practical calculations, it is most convenient to rotate the C_p contour to the imaginary w axis.

The real power of the Wichmann-Kroll method lies in the ease with which the radial Green's functions can be constructed. The following theorem⁷ is all we need: Let $\psi_R(r)$ and $\psi_I(r)$ be the regular and irregular solutions of the radial Dirac equation, $(H - \omega)\psi = 0$, where $(H - \omega)$ is the matrix in eq. (18). The regular solution is that one which is integrable near $r \rightarrow 0$, while the irregular solution is the one which is integrable at $r \rightarrow \infty$. The Green's function is then

$$G_k(r, r'; \omega) = \frac{1}{W(\omega)} \left\{ \theta(r'-r) \psi_R(r) \psi_I^+(r') + \theta(r-r') \psi_I(r) \psi_R^+(r') \right\}, \quad (22)$$

where the $W(\omega)$ is the Wronskian given by

$$W(\omega) = r^2 \left\{ \psi_{R2}(r) \psi_{I1}(r) - \psi_{R1}(r) \psi_{I2}(r) \right\}. \quad (23)$$

It is easy to verify that eq. (22) does satisfy eq. (18). For the trace needed in eq. (21),

$$\text{Tr } G_k(r, r; \omega) = \psi_I^+(r) \psi_R(r) / W(\omega). \quad (24)$$

An important example of the above construction is for the case of a pure Coulomb potential $Z\alpha V(r) = -Z\alpha/r$. The solutions^{8,11} are $\psi_R(r) = M(r)$ and $\psi_I(r) = W(r)$, where M involves linear combinations of regular Whittaker functions $M_{\nu, \pm 1/2, S}(2cr)$ and W involves linear combinations of the irregular Whittaker functions $W_{\nu, \pm 1/2, S}(2cr)$.

The parameters on which M and W depend are $S = \sqrt{k^2 - (Z\alpha)^2}$, $c = \sqrt{m_0^2 - \omega^2}$, and $\nu = Z\alpha/c$. Whittaker functions are related to confluent hypergeometric functions for which rapid, high precision numerical techniques are readily available¹¹. The most important parameter in the case of strong fields ($Z\alpha > 1$) is $S = \sqrt{1 - (Z\alpha)^2}$ for $k = +1$, $j = 1/2$, states. At $Z\alpha = 1$, S and consequently M have a branch point as a function of $Z\alpha$ for $j = 1/2$. Although it seems that W would also have a branch point at $Z\alpha = 1$, $W_{\nu, \pm 1/2, S}$ is an even function of S and therefore nonsingular at $Z\alpha = 1$. It is the nonanalytic behavior of the M function that causes a singularity of $\text{Tr} G_{k=+1}$ for this point nuclear charge case at $Z\alpha = 1$. Higher angular momentum states ($j \geq 3/2$) are, on the other hand, well behaved near $Z\alpha = 1$. Therefore, to extend $Z\alpha$ beyond 1, it is necessary to include finite size corrections for the $j = 1/2$ contribution to the VP density. As we shall see, it is also sufficient to modify only the $j = 1/2$ case.

In order to include finite nuclear size, a definite nuclear model must be adopted. The simplest finite size nuclear density is a shell distribution, for which $V(r) = -1/R$ for $r < R$ and $V(r) = -1/r$ for $r > R$, R being the nuclear radius. With this model it is possible to solve the problem analytically⁸. For $r < R$, the solutions are $j(r)$ and $h(r)$, simply related to spherical Bessel functions. For $r > R$, the Coulomb M and W solutions apply. Continuity at $r=R$ determines the particular linear combination of M and W that joins the interior $j(r)$ solution giving the regular solution. Continuity at $r=R$ also determines that linear combination of the j and h solutions that join the exterior W function that gives the irregular solution. With these solutions for finite nuclear systems, eq. (24) yields⁸

$$\text{Tr}G_k(r, r; \omega) = \begin{cases} \text{Tr}G_k^0(r, r; \omega) + \text{Tr}\Delta G_k^<, & r < R \\ \text{Tr}G_k^{\text{Coul}}(r, r; \omega) + \text{Tr}\Delta G_k^>, & r > R \end{cases} \quad (25)$$

where G_k^0 is the free radial Green's function, G_k^{Coul} is the point nucleus Coulomb Green's function, and $\Delta G_k^{< >}$ are finite size correction functions. Explicit formulas are given in Ref. (8c). It is straightforward to show that $\text{Tr}G_k \rightarrow \text{Tr}G_k^0$ if $R \rightarrow \infty$, while $\text{Tr}G_k \rightarrow \text{Tr}G_k^{\text{Coul}}$ if $R \rightarrow 0$. Furthermore, for $Z < 137$, a useful analytic expression for ΔG_k can be derived by setting the electron mass to zero¹². With this approximation, the contour integration in eq. (19) for the $\text{Tr}G_k$ part can be performed analytically. In this way, the finite size correction to the vacuum polarization potential is found to be¹²

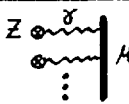
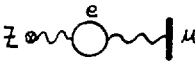
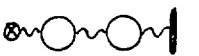
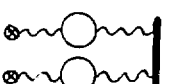
$$\Delta V(r) = \frac{\alpha(Z\alpha)}{15-r} \left(\frac{R}{r}\right) \sqrt{1-(Z\alpha)^2} f[(Z\alpha)^2] \quad (26)$$

valid for $r > R$ and $Z\alpha < 1$. Eq. (26) is particularly useful in computing finite size VP corrections for muonic atoms.

MUONIC ATOMS

High Z muonic atoms provide a good test of vacuum polarization since typical 4f, 5g muonic radii are ~ 50 fm, which satisfy $R \ll a \ll r_e$. Hence, these orbits are insensitive to nuclear details but probe the structure of the vacuum polarization cloud. Furthermore, since $m_\mu \gg m_e$ self-energy corrections are small. The example of muonic Pb is listed in table 1. The contributions to the energy levels were taken from the compilation in Ref. 13. The latest experimental results are in agreement with theory. Comparing the contribution $\Delta E_{3^+} = 45$ eV, due to

Table 1. Contributions¹³ to Energy Levels in Muonic Pb (eV)

Diagram	Order	$4f_{7/2}$	$5g_{9/2}$
1. 	$\alpha^0(Z\alpha)^{n \geq 1}$	-1188318	-758970
2. 	$\alpha^1(Z\alpha)^1$	-3664	-1565
3. 	$\alpha^1(Z\alpha)^{n \geq 3}$	+104	+59
4. 	$\alpha^1(Z\alpha)^{n \geq 1}$	+10	+3
5. 	$\alpha^2(Z\alpha)^1$	-25	-11
6. 	$\alpha^2(Z\alpha)^2$	-9	-3
7. 	$\alpha^2(Z\alpha)^2$	-1	0
8. Nuclear + Atomic Effect		-97	-173

$\Delta E(5g_{9/2} - 4f_{7/2}) = 431,332 \pm 5$ eV	theory
$431,331 \pm 8$ eV	Dubler, et al. ¹⁴
$431,360 \pm 11$ eV	Tauscher, et al. ¹⁵

non-linear vacuum polarization (line 3) with the experimental uncertainties (± 10 eV), we can say that the current experiments test and confirm non-linear vacuum polarization effects at the level of $\sim 20\%$. Encouraged by this success, we now push the theory beyond $Z=137$ up to Z_c .

NON-LINEAR SCREENING AS $Z \rightarrow Z_c$

For a point charge, Wichmann and Kroll showed that the non-linear vacuum polarization density has the form

$$\rho_{VP}^{3+}(r) = Q_{wk}^{3+} \delta(r)/4\pi r^2 + \tilde{\rho}_{wk}^{3+}(r) \quad , \quad (27)$$

where Q_{wk}^{3+} is a point screening charge at the origin and $\tilde{\rho}_{wk}^{3+}$ is a finite compensating VP charge density extending to $r \sim r_{wk}^{3+}$. The net charge of ρ_{VP}^{3+} is, of course, zero. As a function of $Z\alpha$, they found that

$$Q_{wk}^{3+} = -|e| \left\{ (Z\alpha)^3 (0.021) + (Z\alpha)^5 (0.007) F[(Z\alpha)^2] \right\} \quad , \quad (28)$$

where F is close to 1 except near $Z\alpha = 1$. In the limit $Z\alpha \rightarrow 1$, $Q_{wk}^{3+} \rightarrow e/20$, approximately. However, due to the nonanalytic behavior of the $j=1/2$ Green's function at $Z\alpha = 1$, they found that $dQ_{wk}^{3+}/dZ \rightarrow \infty$ at $Z\alpha=1$. The contribution of higher partial waves ($j > 3/2$) to Q_{wk}^{3+} was found^{8,12b} to be less than 10% over the entire range $Z \leq 137$. Almost all the screening charge, therefore, is due to $j=1/2$ pairs.

This last observation greatly simplifies the calculations of ΔE^{3+} for $Z > 137$. To high accuracy, we need only include finite size effects in the $j=1/2$ term, while continuing to use the point charge form of ρ_j^{3+} for $j > 3/2$ (valid up to $Z\alpha = 2$). In table 2, the energy shift^{8b} of the $i s_{1/2}$ state due to non-linear vacuum polarization is given for $Z = Z_c$. The nuclear charge density was taken to be a shell of radius $R = 10$ fm. While the energy shift increases very rapidly for $Z > 137$, $\Delta E^{3+}(Z) \sim Z^{10}$, we see that it nevertheless remains small (≤ 1 keV) and nonsingular as $Z \rightarrow Z_c$. Also, it can be seen that the third order, $(Z\alpha)^3$, contribution accounts for about one-half the repulsion.

It is important to compare these numbers to the first order Uehling shift, which is attractive and hence of opposite sign to ΔE^{3+} . From eq. (16) a simple estimate of ΔE^1 can be made¹³ by replacing $1/r$ by $\langle 1/r \rangle_{1S}$ as listed in table 2. For $Z \rightarrow Z_c$, we get in this way $\Delta E^1 \sim -10$ keV. Detailed calculations¹⁶ give in fact $\Delta E^1(Z_c) = -11.8$ keV. Therefore, $\Delta E^{3+}(Z_c) \approx -\Delta E^1(Z_c)/10$, and the net effect of vacuum polarization to all orders in $Z\alpha$ is attractive at the critical charge! Diving, $B \sim 2m_e$, is therefore enhanced by vacuum polarization.

An interesting way to characterize the effect of non-linear vacuum polarization is to define an effective point screening charge Q_{eff}^{3+} such that

$$\Delta E^{3+} = Q_{eff}^{3+} \langle 1/r \rangle_{1S} \quad . \quad (29)$$

Table 2. Energy Shift (eV) Due to Non-linear Vacuum Polarization for $R = 10$ fm Nuclear Shell Density

Z	$E(1s_{1/2})/m_e c^2$	$\langle r^{-1} \rangle_{1s}$	ΔE^{3+}	ΔE^3	Q_{eff}^{3+}	Q_{eff}^3
82	0.79	0.8	2	2	6×10^{-4}	6×10^{-4}
130	0.362	2.1	63	47	8×10^{-3}	6×10^{-3}
153	-0.137	4.2	307	197	2.0×10^{-2}	1.3×10^{-2}
165	-0.550	5.9	641	368	2.9×10^{-2}	1.7×10^{-2}
175	-0.990	7.6	1140	566	4.1×10^{-2}	2.0×10^{-2}
175	-0.999	7.6	1150	570	4.1×10^{-2}	2.0×10^{-2}

Since $\langle r^{-1} \rangle_{1s} = -dE_{1s}/dZ = dB_{1s}/dZ$, we can determine Q_{eff} from

$$Q_{\text{eff}}^{3+} = -\Delta E^{3+} / (dE_{1s}/dZ) \quad (30)$$

Similarly, we can define an effective third order screening charge using ΔE^3 . The resulting screening charges are illustrated as a function of Z in Fig. 2.

The rapid increase of screening as $Z \rightarrow Z_c$ is obvious. However, the magnitude of $Q_{\text{eff}}^{3+} \approx 0.04e$ remains much smaller than the nuclear charge even at Z_c . Furthermore, dQ_{eff}^{3+}/dZ remains finite at Z_c . Also shown for comparison is the Wichmann-Kroll charge, eq. (28), obtained for a point nuclear density. The small contribution of higher angular momenta ($j \geq 3/2$) at $Z = 137$ is indicated by Q_{eff}^{3+} . Qualitatively, it is suggestive to say that finite nuclear size simply shifts the $Q_{\text{wk}}(Z)$ curve to higher Z: $Q_{\text{eff}}^{3+}(Z) \approx Q_{\text{wk}}(Z - Z_c + 137)$. Note also that for $Z > 137$, $Q_{\text{eff}}^{3+}(Z) \approx Q_{\text{wk}}(Z)$ because for lower Z, the $1s_{1/2}$ radius lies outside the vacuum polarization cloud, and the compensating density ρ_{wk} in eq. (27) shields the VP point charge, Q_{wk} .

In conclusion, non-linear vacuum polarization is nonsingular and small compared to the linear (Uehling) effect in $Z \rightarrow Z_c$.

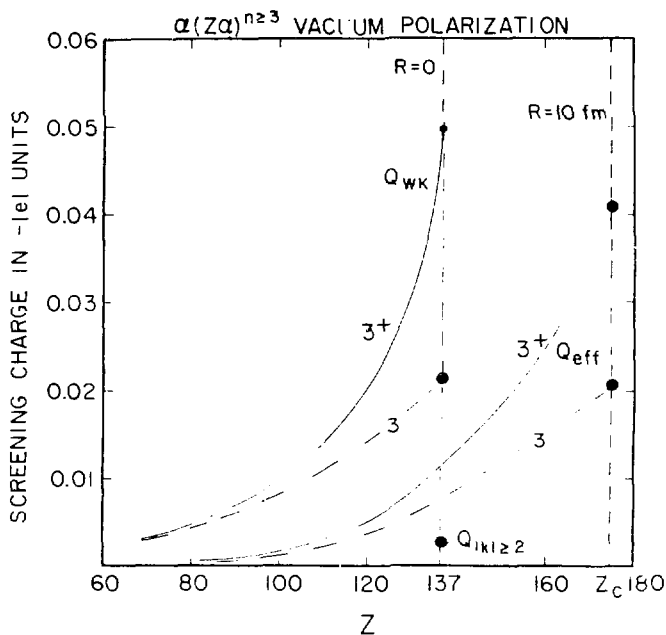


Fig. 2. Effective non-linear screening charge for orders $\alpha(Z\alpha)^{n \geq 3}$ labeled 3^+ and order $\alpha(Z\alpha)^3$ labeled 3 .

Therefore, virtual pair creation does not prevent real pair creation for $Z > Z_c$.

CHARGED VACUUM FOR $Z > Z_c$

For $Z > Z_c$, the $1S_{1/2}$ pole in Fig. 1 moves off the physical sheet through the branch point at $\lambda = -m_0$. The original contour integration over C_F is then no longer well defined beyond Z_c . Therefore, ψ_p is nonanalytic at $Z = Z_c$, although the limit $Z \rightarrow Z_c$ from below ψ_p remains small and nonsingular. The nonanalytic behavior signals a breakdown in the assumption that the chargeless vacuum state is the one of lowest energy. Beyond Z_c , $B = 2m_0$ and the state with two electrons bound around the nucleus and two free positrons has lower energy and will therefore define the new vacuum¹⁻³.

We expect therefore that the vacuum charge density ρ_{VP} should be a smooth continuation of the helium-like density $2e|\psi_{1S1/2}(x)|^2$. However, the $1S_{1/2}$ state no longer exists as part of the Dirac spectrum for $Z > Z_c$. This poses no difficulty, however, if we realize that the physical helium-like density includes the vacuum polarization cloud:

$$\begin{aligned} \rho_{He}(x) &= 2e|\psi_{1S1/2}(x)|^2 + \rho_{VP}(x) \\ &= |e| \int_{C_{He}} \frac{d^4x}{2\pi^4} \text{Tr } G(x, x; -) \end{aligned} \quad (31)$$

where C_{He} is the contour C_F shifted to the right of the $1S_{1/2}$ pole in Fig. 1. For $Z \leq Z_c$ the first line is well defined. However, the contour integral is perfectly well defined both below and above Z_c . It is manifestly analytic in Z in the neighborhood of Z_c . Therefore, the contour integral representation allows⁸ us to compute the continuation of the helium-like density and hence the overcritical vacuum density for $Z > Z_c$. (The Green's function must, of course, be regulated as in eq. (12) for all Z .) The highly localized character of the overcritical charged vacuum density is shown in Fig. 3. In this example, the $1S_{1/2}$ state dives at $Z_c \approx 1.274$. However, we can see that the vacuum density defined by eq. (31) for $Z > Z_c$ is a smooth analytic continuation of the He-like density from $Z < Z_c$ all the way up to the diving point of the $2P_{1/2}$ state. Finally, the smooth increase in the localization of the vacuum density beyond Z_c can be seen from the average inverse radius in Fig. 3b.

SUMMARY

In this review, I have shown how the Wichmann-Kroll formalism can be applied to finite radius nuclei with very large Z . The non-linear vacuum polarization was shown to remain too small to prevent spontaneous pair production for $Z > 175$. Finally, the density of the overcritical charged vacuum was shown to be highly localized and continuous up to the $2P_{1/2}$ diving point.

This work was supported by the Director, Office of Energy Research, Division of Nuclear Physics of the Office of High Energy and Nuclear Physics of the U.S. Department of Energy under Contract W-7405-ENG-48.

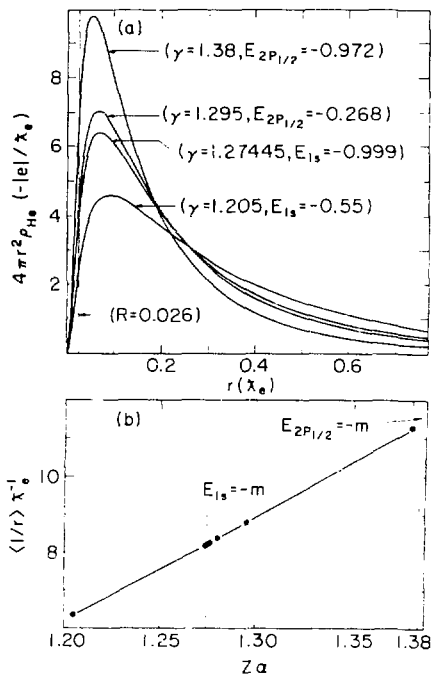


Fig. 3. a) Charge density of He-like state which corresponds to the vacuum density for $Z = 1.275$.
b) Average inverse radius of He-like state.

REFERENCES

1. W. Pieper, W. Greiner, Z. Phys. 218:227 (1969).
2. B. Muller, J. Rafelski, W. Greiner, Z. Phys. 257:62 (1972); Z. Phys. 257, 83 (1972); Nucl. Phys. B68:585 (1974).
3. Ya.B. Zel'Dovich, V.S. Popov, Sov. Phys. Usp. 14:673 (1972).
4. J. Rafelski, L.P. Fulcher, W. Greiner, Phys. Rev. Lett. 27:958 (1971).
5. M. Born, L. Infeld, Proc. Roy. Soc. (London) A144:425 (1934).
6. G. Soff, J. Rafelski, W. Greiner, Phys. Rev. A7:903 (1973).
7. E.H. Wichmann, N.M. Kroll, Phys. Rev. 96:232 (1954); 101, 843 (1956).

8. M. Gyulassy, (a) Phys. Rev. Lett. 32:1393 (1974), (b) Phys. Rev. Lett. 33:921 (1974), (c) Nucl. Phys. A244:497 (1975).
9. J.D. Bjorken, S.D. Drell, "Relativistic Quantum Fields," vols. I,II (McGraw-Hill, New York, 1965).
10. J. Blomquist, Nucl. Phys. B48:95 (1972).
- 11a. P.J. Mohr, Phys. Rev. Lett. 34:1050 (1975); Ann. Phys. (N.Y.) 88:26, 52 (1974);
b. K.T. Cheng, W.R. Johnson, Phys. Rev. A14:1943 (1976).
- 12a. J. Arafune, Phys. Rev. Lett. 32:560 (1974);
b. L.S. Brown, R.N. Cahn, L.D. McLerran, Phys. Rev. Lett. 32:562 (1974); Phys. Rev. D12, 609 (1975).
13. S.J. Brodsky, P.J. Mohr, in "Structure and Collisions of Ions and Atoms," I.A. Sellin, ed., New York, Springer (1978).
14. T. Dubler, K. Kaesser, B. Robert-Tissot, L.A. Schaller, L. Schellenberg, H. Schenewly, Nucl. Phys. A294:3+7 (1978).
15. L. Tauscher, G. Backenstoss, K. Fransson, H. Koch, A.Nilsson, J. de Raedt, Z. Phys. A285:139 (1978).
16. G. Soff, B. Müller, J. Rafelski, Z. Naturforsch A29:1267 (1974).